

An Analysis of 3D Solvation Structure in Biomolecules: Application to Coiled Coil Serine and Bacteriorhodopsin

Kenji Hirano,[†] Daisuke Yokogawa,[‡] Hirofumi Sato,^{*,†} and Shigeyoshi Sakaki^{†,§}

Department of Molecular Engineering, Kyoto University, Kyoto 615-8510, Japan, and Institute for Protein Research, Osaka University, Osaka 565-0871, Japan

Received: December 3, 2009; Revised Manuscript Received: February 2, 2010

Three-dimensional (3D) solvation structure around coiled coil serine (Coil-Ser) and inner 3D hydration structure in bacteriorhodopsin (bR) were studied using a recently developed method named multicenter molecular Ornstein–Zernike equation (MC-MOZ) theory. In addition, a procedure for analyzing the 3D solvent distribution was proposed. The method enables us to calculate the coordination number of solvent water as well as the strength of hydrogen bonding between the water molecule and the protein. The results for Coil-Ser and bR showed very good agreement with the experimental observations.

Introduction

It is well established that the solvent effect has an essential role in a biomolecular system such as protein.¹ The function and structure can not be explained without considering the effect of the surrounding and/or inside water molecules. One of the representative examples is water in Bacteriorhodopsin (bR), which is a light-driven proton pump in *Halobacterium salinarum*,² where the proton transfer is accomplished by the hydrogen bonding networks of the inner water molecules around the Schiff base. High resolution X-ray crystallography,³ Fourier transform infrared spectroscopy (FT-IR),⁴ and quantum mechanics/molecular mechanics (QM/MM) calculations⁵ have been performed to elucidate the mechanism of pump, namely, the role of these water molecules on the proton pathway.

bR is rather the exception, and understanding the solvent effect is still very limited despite its significant importance. Coiled coil serine (Coil-Ser)⁶ belongs to an α helical coiled-coil motif.⁷ It was originally designed to provide a model system for evaluating the helix-forming tendency and expected to form a parallel dimer. Actually, however, it has three α helices, and one of them is in the antiparallel direction relative to the others. The formation looks unstable in terms of the electrostatic interaction between helices because the residues charged with the same sign approach each other. A large number of mutations have been performed, and several hypotheses have been proposed^{8–10} to explain the unexpected structure; for example, to avoid the steric clash of tryptophans, hydrogen bonds between protonated and deprotonated glutamic acids and so on. It should be pointed out that the solvent effect has not been appropriately discussed so far, presumably because of the absence of reliable information of the solvation structure, which is indispensable to understand the stability of the protein.

Computation of accurate 3D solvation structure, in general, is very time-consuming. Molecular dynamics (MD), which is mostly used for studying a biomolecular system, requires numerous computational times to obtain adequate 3D solvation structure. An integral equation theory for the molecular liquid,

the 3D reference interaction site model (3D-RISM),^{11,12} succeeds in providing accurate solvent distribution with a reasonable computational cost, and in revealing the role of solvent water in various systems.^{13–16} The method involves time-consuming 3D fast Fourier transformation (3D-FFT), which makes the parallelization difficult. Yokogawa et al. recently developed another integration theory that enables us to efficiently compute 3D solvation structure (MC-MOZ; multicenter molecular Ornstein–Zernike equation theory^{17,18}). While both 3D-RISM and MC-MOZ give essentially the same results as shown in the previous study, MC-MOZ does not require 3D-FFT and highly efficient parallelization is achieved.

Now, a reliable 3D structure becomes available, which provides the understanding of the solvation effect in an intuitive manner. Although a quantitative analysis in which 3D solvation structure is converted into a radial distribution function was reported,¹⁹ there are still very few analysis methods. The present situation prompts us to develop a quantitative analysis. Recently, Matsuoka et al. reported the computistical probability distribution of hydration water molecules around polar atoms in a huge number of entries in the protein data bank (PDB). The Gaussian fitting method was applied for quantitative analysis of the distribution in terms of the peak positions and the widths.²⁰ Here, we propose an analysis to directly characterize the 3D distribution function obtained by the first principle calculations. The method enables us to calculate the coordination number of water molecules as well as to analyze the fluctuation of the localized distribution. The purpose of the present work is to characterize 3D solvation structure around protein. As an illustration, two proteins (bR and Coil-Ser) were chosen to demonstrate newly developed MC-MOZ and the analysis method. We note that these two systems are representatives of a different category of 3D solvation structure, i.e., the “inside” (bR) and “outside” (Coil-Ser) water.

Method

A. Multicenter Molecular Ornstein–Zernike Equation (MC-MOZ) Theory. Since the details of the theory were described elsewhere,^{17,18} only the outlines are explained. 3D total correlation function in the theory, H_α , is expressed as the sum of the reference (H_α^{ref}) and residual (ΔH_α) correlation functions,

* Corresponding author. E-mail: hirofumi@moleng.kyoto-u.ac.jp.

[†] Kyoto University.

[‡] Osaka University.

[§] Fukui Institute for Fundamental Chemistry, Kyoto University, Takano-Nishihiraki-cho 34-4, Sakyo-ku, Kyoto 606-8103, Japan.

$$H_\alpha(\mathbf{r}) = H_\alpha^{\text{ref}}(\mathbf{r}) + \Delta H_\alpha(\mathbf{r}) \quad (1)$$

where α indicates solvent site. 3D direct correlation function, C_α , is divided into two terms in a similar manner. While the reference correlation functions, H_α^{ref} and C_α^{ref} , are defined as 1D functions, the residual correlation terms are further divided into the components on each site in the solute and expanded with real solid harmonics in 3D. The equations are solved by coupling with the closure equation such as Kovalenko–Hirata type.^{17,18,21} Finally, the 3D solvation structure $G_\alpha(\mathbf{r})$ is obtained from H_α ,

$$G_\alpha(\mathbf{r}) = H_\alpha(\mathbf{r}) + 1 \quad (2)$$

$G_\alpha(\mathbf{r})$ represents the probability to find α -site (i.e., the oxygen or hydrogen in the case of water) of solvent at the position of \mathbf{r} .

B. Analysis of 3D Solvation Structure. The coordination number of water molecules, N_w , is a fundamental quantity and defined as

$$N_w = \rho_w \int \int \int_V G_O(x,y,z) dx dy dz \quad (3)$$

ρ_w represents the number density of solvent water and the integration was numerically performed using Simpson's formula. The cuboid integral volume V was taken around the peak of the 3D distribution; its boundary was set at the local minima of the 3D function as close as possible. This is an analogue to the calculation procedure of the coordination number from 1D radial distribution function.

The most fundamental quantity to characterize a distribution is its mean value and deviation. In the present case, the former corresponds to the peak position, and the latter is deeply related to the fluctuation of water molecules. Let us assume that 3D solvation structure is well localized, and the water molecule fluctuates around a specific point just like a harmonic oscillator. Then a Gaussian function best describes the distribution, and its exponent (σ) characterizes the fluctuation. In general, the center of the distribution is not located at the origin and the directions of the anisotropy axis are not necessary to coincide with that of the spatial coordinate system. Hence, the distribution is expressed using a set of nonspherical Gaussian functions as follows,

$$\begin{aligned} \tilde{G}_\alpha(x,y,z) &= \sum_i^N \tilde{G}_{\alpha,i}(x,y,z) \\ &= \sum_i^N B_i \exp \left[-\frac{1}{2} \left\{ \frac{(x-x_i)^2}{\sigma_{1,i}^2} + \frac{(y-y_i)^2}{\sigma_{2,i}^2} + \frac{(z-z_i)^2}{\sigma_{3,i}^2} + \right. \right. \\ &\quad \left. \left. \frac{(x-x_i)(y-y_i)}{\sigma_{4,i}^2} + \frac{(y-y_i)(z-z_i)}{\sigma_{5,i}^2} + \frac{(z-z_i)(x-x_i)}{\sigma_{6,i}^2} \right\} \right] \end{aligned} \quad (4)$$

where N is the number of Gaussian function for the expansion. In eq 4, the distribution corresponding to each Gaussian ($\tilde{G}_{\alpha,i}$) is described by ten parameters including the center (x_i , y_i , z_i), prefactor B_i , and a set of σ 's. They can be determined by minimizing χ^2 ,

$$\chi = G_\alpha(x,y,z) - \tilde{G}_\alpha(x,y,z) \quad (5)$$

It is always possible to transform $\tilde{G}_{\alpha,i}$ in eq 4 into a simpler expression by properly rotating the spatial coordinate system using standard Eulerian angles, ψ , θ , and ϕ .

$$B_i \exp \left[-\frac{1}{2} \left\{ \left(\frac{x'-x_i}{\sigma_{x_i}} \right)^2 + \left(\frac{y'-y_i}{\sigma_{y_i}} \right)^2 + \left(\frac{z'-z_i}{\sigma_{z_i}} \right)^2 \right\} \right] \quad (6)$$

In our actual procedure, the nonspherical Gaussian function is transformed so as to minimize χ^2 ; namely, it is shifted by changing the center (x_i , y_i , z_i), rotated by changing the Eulerian angles (ψ , θ , and ϕ), and reshaped by fitting three σ 's and B_i . The distribution is again described by ten parameters. Three axes of the obtained distribution correspond to the direction of the solvent fluctuations. Different from the recent work by Matsuoka et al.,²⁰ we directly fit the computed solvent distribution to 3D Gaussian function. The fitted Gaussian function may be related to the Boltzmann distribution of the potential energy of the harmonic oscillator, E_x , E_y , and E_z .

$$\begin{aligned} \exp \left[-\frac{1}{2} \left\{ \left(\frac{x'-x_i}{\sigma_{x_i}} \right)^2 + \left(\frac{y'-y_i}{\sigma_{y_i}} \right)^2 + \left(\frac{z'-z_i}{\sigma_{z_i}} \right)^2 \right\} \right] \propto \\ \exp \left[\frac{-(E_x + E_y + E_z)}{k_B T} \right] \end{aligned} \quad (7)$$

Looking at both sides, “force constant” and “frequency” can be defined for each water molecules, for example, the x component of the i th Gaussian is

$$k_{x_i} = \frac{k_B T}{\sigma_{x_i}^2} \quad \tilde{v}_{x_i} = \frac{1}{2\pi c} \sqrt{\frac{k_{x_i}}{m}} = \frac{1}{2\pi c \sigma_{x_i}} \sqrt{\frac{k_B T}{m}} \quad (8)$$

where c and m are the speed of light and the mass of a water molecule, respectively. \tilde{v}_x basically represents the curvature of the energy surface, that is to say, how strongly water molecules are localized. We call this wavenumber the “fluctuation wavenumber” in the paper. It is noted that the number represents the localization of a water molecule arising from any kind of interaction between protein and solvent water including hydrogen bonding, van der Waals interactions, and so on, although the hydrogen bonding is primarily important in many cases of the present study.

Computational Details

The structure of Coil-Ser and bR were taken from the PDB data (1COS⁶ and 1C3W³). Amber 99²² and OPLS²³ were employed for the intermolecular potential of Coil-Ser, and bR, respectively. SPC-like water²⁴ was used with a correction concerning the Lennard-Jones parameters of the hydrogen sites ($\sigma = 1.0 \text{ \AA}$, $\epsilon = 0.056 \text{ kcal mol}^{-1}$). The number of grid points in this work for MC-MOZ calculations is 512 for the radial part and 194 for the angular part on each solute atom. The maximum number of the real solid harmonics was 10 for the expansion of the residual correlation functions. The temperature and number density of solvent water were 298.15 K and 0.033 426 \AA^{-3} , respectively. To visualize 3D solvation structure, VMD software²⁵ was used.

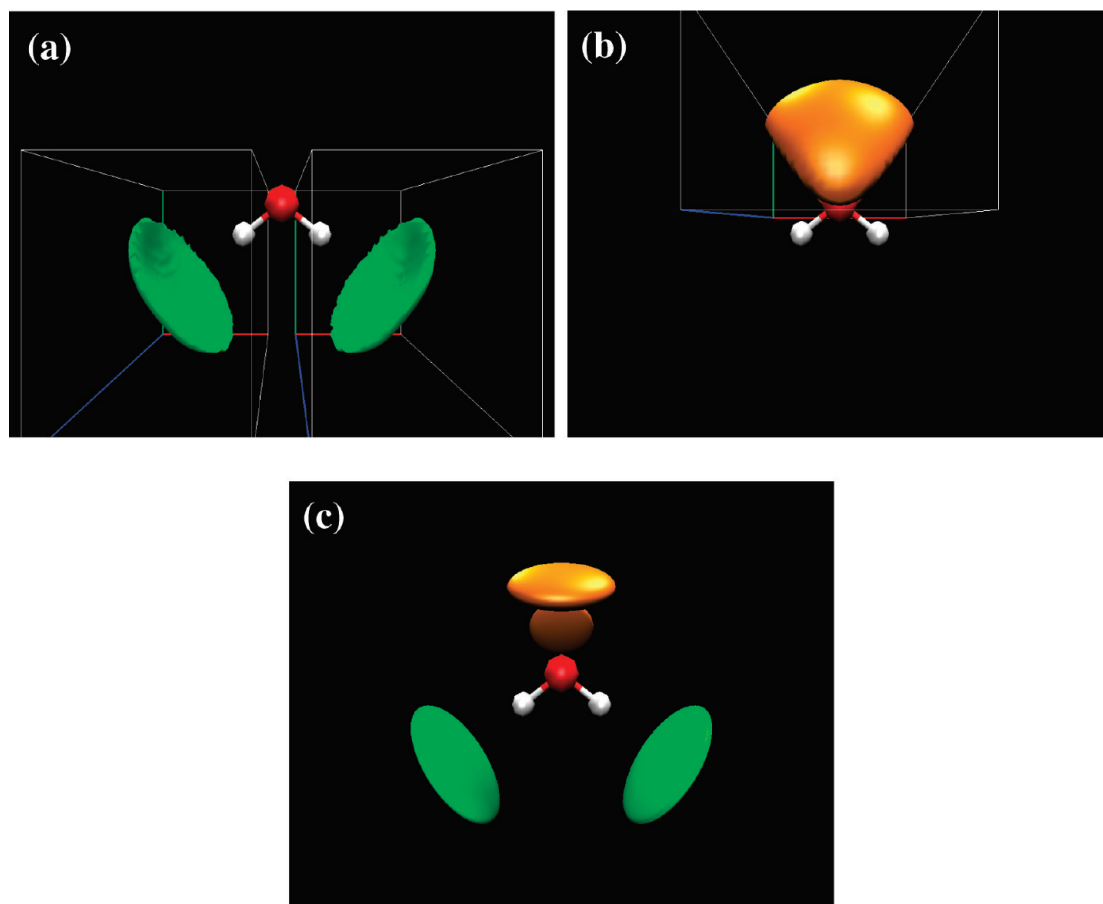


Figure 1. 3D solvation structure of water (a) oxygen (green) and (b) hydrogen (orange) in liquid water. (c) Fitted Gaussian functions.

Results and Discussion

Liquid Water. Before going to the proteins, 3D solvation structure of a water molecule in liquid water is demonstrated. The distributions of oxygen and hydrogen obtained by MC-MOZ are respectively shown in Figure 1a,b with thresholds of 2.8 (oxygen) and 1.8 (hydrogen). The results correspond to the tetrahedral hydrogen bonding network in liquid water. By performing the integration in the boxes shown in the figures, we obtain the coordination numbers 1.26 (oxygen) and 0.99 (hydrogen). The oxygen number slightly includes the contribution from the second solvation area, but both of these values clearly show the reliability of the method. Figure 1c displays the fitted Gauss functions. In the present study, the distribution of a water molecule is described by single Gaussian function; Since the targeted distribution of oxygen consists of two water molecules, two Gaussian functions were prepared for the description.

The standard deviation of these Gaussians corresponding to the three directions are respectively 2.85, 0.50, and 2.71 \AA^2 for oxygen (O_w), and 1.50, 0.43, and 1.37 \AA^2 for hydrogen (H_w). Their fluctuation wavenumbers are 6.9, 39.2, and 7.3 cm^{-1} for O_w , and 13.1, 46.0, and 14.4 cm^{-1} for H_w . Note that the number is closely related to the strength of hydrogen bonding between water molecules, and the directions of the largest ones (39.2 and 46.0 cm^{-1}) correspond to that of hydrogen bonding.

Coil-Ser. In Figure 2, 3D solvation structure of water around Coil-Ser is shown. The protein is displayed by red, blue, light blue, and white spheres, respectively, corresponding to oxygen, nitrogen, carbon, and hydrogen atoms of lysines. Other residues are represented by gray spheres. The distribution function of water hydrogen and oxygen sites calculated by MC-MOZ ($G_\alpha(\mathbf{r})$

≥ 3.0) are depicted with the orange and green meshed areas, together with the positions of water molecules determined by X-ray crystallography⁶ (small red spheres). In comparing theoretical and experimental results, we note that, different from the green wire frames, the orange ones should be found only in the case when the orientation of a water molecule is relatively fixed, corresponding to a coordinating (hydrating) water molecule. Thus, the combinations of these wire frames are important to see the hydration of water molecule. As shown in Figure 2, the computed distribution shows good agreement with the experimentally obtained water positions because the green-orange combinations are close to almost all positions of X-ray waters (red circles). These water molecules seem to form hydrogen bonds, where the direction of the O–H bond is considerably localized; i.e., rotational fluctuation becomes rather suppressed. It should be mentioned that the temperature effect is directly treated in the present method, and the computed distribution area should be larger than the experimental one due to the thermal fluctuation. The distribution is often found in vacant spaces between residues due to the van der Waals interaction. Because of the hydrophilic interaction, the distribution of water oxygen tends to be found in the vicinity of nitrogen and oxygen atoms of the protein. On the other hand, there is little distribution around hydrophobic sites like the methylene group of the side chain of lysines.

One of the representative distributions is found in the area where the cationic termini of lysines approach each other. Figure 3a focuses on region A, which is enclosed with the white-dashed line in Figure 2, where LYS15 of chain B (LYSII) and LYS15 of chain C (LYSIII) exist. Closely looking at the figure, the water distribution is most likely to coordinate to one of the termini

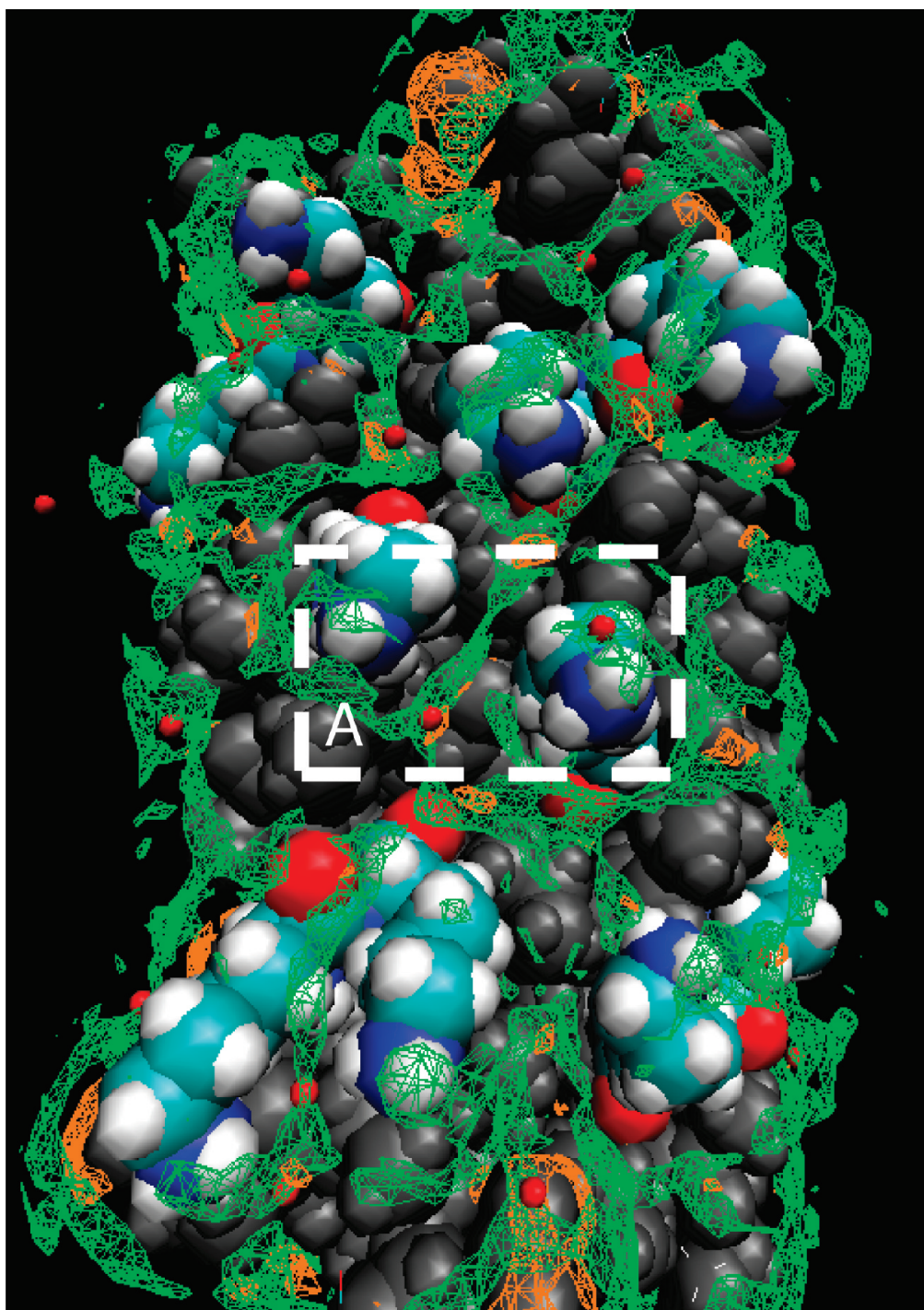


Figure 2. 3D solvation structure around Coil-Ser. The green (orange) regions represent the area where the distribution function of the water oxygen (hydrogen) site is larger than 3.0.

(LYSI) by forming a hydrogen bond. The hydrogen distribution (orange area) neighbors the oxygen distribution, being opposite to LYSI, evidently indicating the hydrogen bonding of LYSI \cdots O_w–H_w. This direction is reasonable when the charge of termini of LYSI is considered. Figure 3b is the same area, but plotted with a higher threshold ($G_a(\mathbf{r}) \geq 5.0$), corresponding to strongly bonded water distribution. By analyzing the distribution function, we determine the boundary box for the integration as depicted in this figure. The computed coordination number in the box is 1.03, corresponding to a water molecule recorded in PDB data (red small sphere, W307). As seen above, W307 is isolated from nearby water molecules and the number is relatively insensitive to the boundary. Hence we may conclude

that the present result is fully consistent with the experimental knowledge. It is interesting to point out that the fluctuation of H_w is considered to be larger than that of O_w, because the distribution is low and flat compared to the oxygen distribution and does not appear with the high threshold. Figure 3c shows the distribution of the fitted Gaussian function (green area). The deviation of each component are respectively 0.32, 0.76, and 1.78 Å and their fluctuation wavenumbers are 61.8, 25.8, and 11.0 cm $^{-1}$, corresponding to the X, Y, and Z directions depicted in the figure. The number toward the X axis is the largest whose direction represents the hydrogen bonding. It is greater than that of liquid water; in other words, the strength of the hydrogen bonding with the protein is greater. The standard deviation of

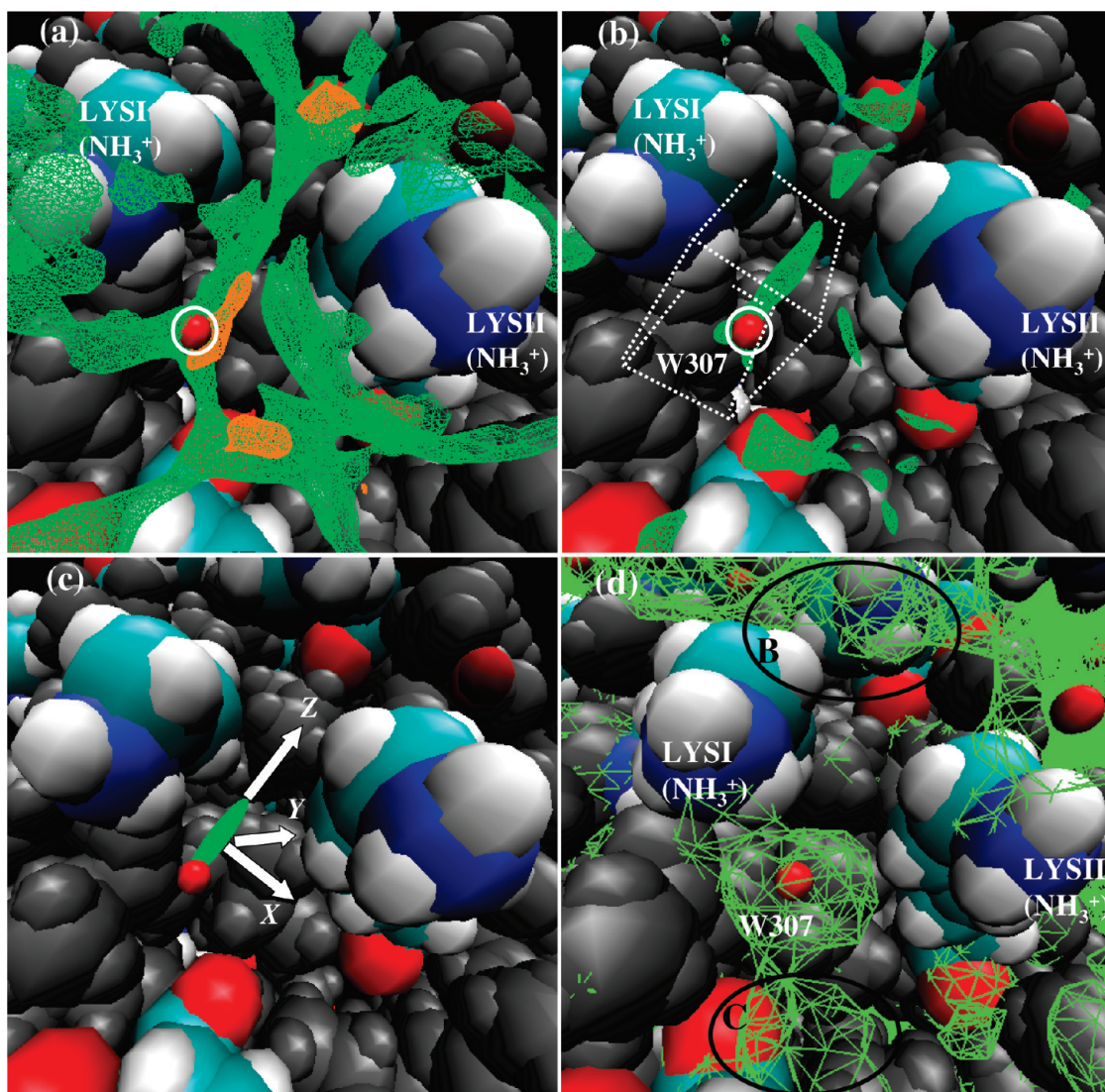


Figure 3. 3D solvation structure around region A. The green (orange) regions represent the area where the distribution function of the water oxygen (hydrogen) site is larger than 3.0 (a) and 5.0 (b). The box in (b) represents the numerical integration area. The Gaussian function is represented by green regions in (c) where the value is larger than 5.0. The lime region in (d) represents the electron density map obtained by X-ray.

the distance distribution between NH_3^+ of lysine and water reported by Matsuoka et al.²⁰ is 0.13–0.14 Å. Our results reasonably agree with their report but are slightly larger. Presumably, it is attributed to the temperature effects because room temperature is assumed in our computations. The present result implies that the electrostatic repulsion between lysine residues is weakened by a strongly bound water molecule, which may be linked to the screening effect of water. Many similar water molecules were found in other electrostatically unfavorable areas. For example, Glu-6 and Glu-13 of chain A and Glu-13 of chain B approach each other (not shown), making this region very unfavorable in terms of the electrostatic repulsion. In the area, water distribution with a high probability is found. On the associating helices, the hydrophobic residues should mainly contribute to the stabilization between helices, but water molecules around Coil-Ser assist the association of the helices by weakening the electrostatic repulsion.

Finally, Figure 3d shows the electron density map taken from the PDB data (lime wireframe). In addition to W307, the computed distribution of atoms (see Figure 3a,b) are near the electron distribution seen in region B and C (Figure 3d).

bR. Some of us already reported that calculated 3D solvation structure was consistent with the experimentally obtained

positions of water molecules and hydrogen bondings.¹⁸ In the present work, the present analysis is applied to quantify the computational results. Figure 4a shows the distribution of water oxygen (green) and hydrogen (orange) around the Schiff base. It is experimentally established that there are three water molecules in this area. The coordination numbers were calculated by dividing the integral range into two regions, V1 and V2. The number in region V1 and V2 are 0.83 and 2.38, respectively, which reasonably agrees with the experimental results though the calculation slightly overestimates the number.

The fitting method was applied to the oxygen distributions in the two regions (Figure 4b). The fluctuation wavenumbers of these Gaussians are shown in Table 1. The number of W402 is the largest (84.2 cm^{-1}) among those of the three water molecules and is also larger than that in liquid water. This indicates that the hydrogen bonding of ASP85 and W402 is stronger than that in liquid water, like the water molecule associated with Coil-Ser. Besides, strong localized hydrogen distribution is found between the W402 oxygen distribution and ASP85. O_w and H_w of W402 lie on a straight line toward the oxygen site of ASP85 to make a strong hydrogen bond. Concerning W402, the shift of the O–D stretching vibration was observed by FT-IR,^{26,27} indicating the formation of strong

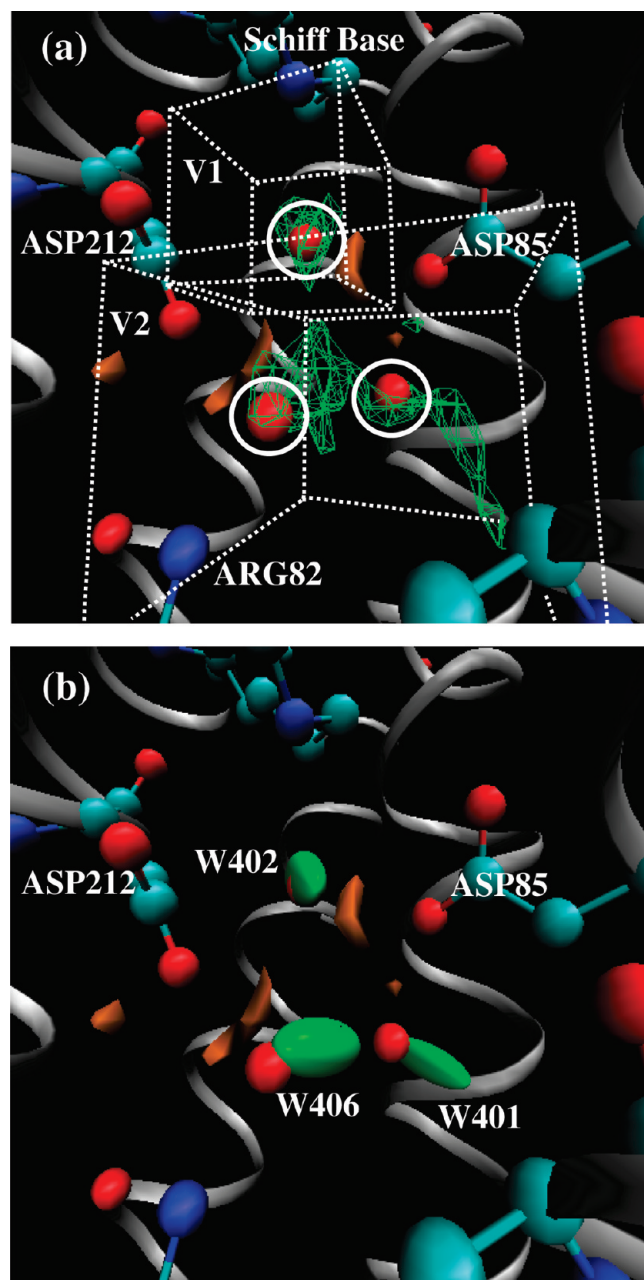


Figure 4. 3D solvation structure of water oxygen (green) and hydrogen (orange) in (a). The threshold of the distribution is 5.0. The boxes are integral areas for calculating coordination numbers. The distribution in these areas is fitted to Gaussian functions as shown in (b).

TABLE 1: Standard Deviation and the Fluctuation Wavenumber of the Fitted Gaussian Functions in bR^a

atom label	σ_{x_i}	σ_{y_i}	σ_{z_i}	$\tilde{\nu}_{x_i}$	$\tilde{\nu}_{y_i}$	$\tilde{\nu}_{z_i}$
W401	0.28	0.31	1.05	69.2	62.9	18.8
W402	0.23	0.33	1.00	84.2	60.3	19.7
W406	0.52	0.59	1.12	38.0	33.1	17.6

^a Given in Å² and cm⁻¹. Because of the arbitrary of the direction, the smallest component in σ (the largest component in $\tilde{\nu}$) is chosen as the x direction.

hydrogen bonding.²⁸ The present calculation about W402 is consistent with the FT-IR. On the other hand, the hydrogen distribution between oxygen of W402 and ASP212 is very small. Actually, the calculated number of the hydrogen site between W402 and ASP212 was 0.40, whereas that between W402 and ASP85 is 0.90. Thus, W402 prefers to form a hydrogen bond

with ASP85 than with ASP212. Such a asymmetric hydrogen bond network has been reported by experiments²⁹ and simulation⁵ and is said to be fundamental for the proton pump function of bR. The present first principle study suggests that W402 makes the strongest hydrogen bond with bR in the Schiff base region in which an asymmetric hydrogen bond network is constructed.

Conclusion

A highly parallelizable MC-MOZ theory was applied to compute the 3D solvation structure of biomolecular systems. The solvent distribution shows good agreement with those by X-ray crystallography. The present method directly examines the strength of hydrogen bondings through the 3D solvation structure. The results are in good agreement with the experimentally observed shift change of the spectroscopy. The “fluctuation wavenumber” is a very useful tool to quantify the strength of hydrogen bonding. It is worthwhile to mention that it provides the understanding of solvation picture in a semi-quantitative manner.

One might notice that the fluctuation wavenumber may be related to anisotropic B-factor, which describes the attenuation of X-ray scattering caused by thermal motion corresponding to harmonic oscillator. Unfortunately, the anisotropic B-factor has not been reported for the present systems, prohibiting the direct comparison. It should be noted that the fluctuation of protein, not only the backbone but also the side chain, is not treated in the present work, and the PDB structure is straightforwardly employed. While the method based on integral equation theory for molecular liquids including the present MC-MOZ enables us to compute high-precision 3D solvation structure free from the sampling error, the introduction of the structural fluctuation is quite difficult. The analysis proposed here may be applicable to the structure obtained by molecular simulation such as MD, in which the protein fluctuation is naturally taken into account, but the 3D solvation structure must be accurate because the small sampling errors should cause inaccurate evaluation. The treatment of the structural fluctuation is now in progress and will be reported near future.

Acknowledgment. This work has been financially supported in part by the Grant-in Aid for Scientific Research on Priority Area “Molecular Science of Fluctuations” (2006-21107511) and by the Grant-in Aid for General Research (19350010). All of them were supported by the Ministry of Education, Culture, Sports, Science, and Technology (MEXT) Japan.

References and Notes

- (1) Chaplin, M. *Nat. Rev. Mol. Cell Biol.* **2006**, 7, 861.
- (2) Mathies, R. A.; Lin, S. W.; Ames, J. B.; Pollard, W. T. *Annu. Rev. Biophys. Biophys. Chem.* **1991**, 20, 491.
- (3) Luecke, H.; Schobert, B.; Richter, H. T.; Cartailler, J. P.; Lanyi, J. K. *J. Mol. Biol.* **1999**, 291, 899.
- (4) Kandori, H. *Biochim. Biophys. Acta* **2000**, 1460, 177.
- (5) Hayashi, S.; Ohmine, I. *J. Phys. Chem. B* **2000**, 104, 10678.
- (6) Lovejoy, B.; Choe, S.; Cascio, D.; McRorie, D. K.; DeGrado, W. F.; Eisenberg, D. *Science* **1993**, 259, 1288.
- (7) Lupas, A. *Trends Biochem. Sci.* **1996**, 21, 375.
- (8) Boice, J. A.; Dieckmann, G. R.; DeGrado, W. F.; Fairman, R. *Biochemistry* **1996**, 35, 14480.
- (9) Betz, S.; Fairman, R.; O’Neil, K.; Lear, J.; DeGrado, W. *Philos. Trans. R. Soc. London, B* **1995**, 348, 81.
- (10) Ogihara, N. L.; Weiss, M. S.; DeGrado, W. F.; Eisenberg, D. *Protein Sci.* **1997**, 6, 80.
- (11) Beglov, D.; Roux, B. *J. Phys. Chem. B* **1997**, 101, 7821.
- (12) Kovalenko, A.; Hirata, F. *Chem. Phys. Lett.* **1998**, 290, 237.
- (13) Imai, T.; Hiraoka, R.; Kovalenko, A.; Hirata, F. *J. Am. Chem. Soc.* **2005**, 127, 15334.

- (14) Yoshida, N.; Phongphanphanee, S.; Maruyama, Y.; Imai, T.; Hirata, F. *J. Am. Chem. Soc.* **2006**, *128*, 12042.
- (15) Phongphanphanee, S.; Yoshida, N.; Hirata, F. *Chem. Phys. Lett.* **2007**, *449*, 196.
- (16) Kiyota, Y.; Hiraoka, R.; Yoshida, N.; Maruyama, Y.; Imai, T.; Hirata, F. *J. Am. Chem. Soc.* **2009**, *131*, 3852.
- (17) Yokogawa, D.; Sato, H.; Imai, T.; Sakaki, S. *J. Chem. Phys.* **2009**, *130*, 064111.
- (18) Yokogawa, D.; Sato, H.; Sakaki, S. *J. Mol. Liq.* **2009**, *147*, 112.
- (19) Johnson, R. S.; Yamazaki, T.; Kovalenko, A.; Fenniri, H. *J. Am. Chem. Soc.* **2007**, *129*, 5735.
- (20) Matsuoka, D.; Nakasako, M. *J. Phys. Chem. B* **2009**, *113*, 11274.
- (21) Kovalenko, A.; Hirata, F. *J. Chem. Phys.* **1999**, *110*, 10095.
- (22) Wang, J.; Cieplak, P.; Kollman, P. A. *J. Comput. Chem.* **2000**, *21*, 1049.
- (23) Jorgensen, W. L. OPLS and OPLS-AA Parameters for Organic Molecules, Ions, and Nucleic Acids, Yale University, 1997.
- (24) Berendsen, H. J. C.; Postma, J. P. M.; van Gunsteren, W. F.; Hermans, H. J. In *Intermolecular Forces*; Pullman, B., Ed.; Reidel: Dordrecht, The Netherlands, 1981.
- (25) Humphrey, W.; Dalke, A.; Schulten, K. *J. Mol. Graph.* **1996**, *14*, 33.
- (26) Kandori, H.; Shichida, Y. *J. Am. Chem. Soc.* **2000**, *122*, 11745.
- (27) Shibata, M.; Tanimoto, T.; Kandori, H. *J. Am. Chem. Soc.* **2003**, *125*, 13312.
- (28) Fecko, C. J.; Eaves, J. D.; Loparo, J. J.; Tokmakoff, A.; Geissler, P. L. *Science* **2003**, *301*, 1698.
- (29) Shibata, S.; Kandori, H. *Biochemistry* **2005**, *44*, 7406.

JP911470P